New Combinatorial Approach for the Investigation of Kinetics and Temperature Dependence of Surface Reactions in Thin Organic Films

Alexander Shovsky and Holger Schönherr*

Department of Materials Science and Technology of Polymers, MESA+ Institute for Nanotechnology and Faculty of Science and Technology, University of Twente, P.O. Box 217, 7500 AE Enschede, The Netherlands

Received December 10, 2004. In Final Form: March 1, 2005

In this paper we present a new, simple, and reproducible method for the rapid determination of the temperature dependence of solution phase surface reactions of organic thin films on solid supports. Instead of estimating the extent of reaction for many separate samples for many different temperatures sequentially, we exploit in our new high throughput combinatorial approach surface reactions carried out under a thermal gradient followed by position-resolved contact angle (CA) measurements. The reaction kinetics, activation energies, and entropies are, thus, accessible on the basis of measurements on a very limited set of samples that differ in reaction times. The kinetics and temperature dependence of surface reactions of the previously studied alkaline hydrolysis of 11,11′-dithiobis(*N*-hydroxysuccinimidylundecanoate) (NHS-C10) self-assembled monolayers (SAMs) on gold, as well as the ester hydrolysis in SAMs of the novel disulfide 11,11′-dithiobis(*tert*-butylundecanoate) (*t*-Bu-C10), were investigated in detail using the conventional sequential and the new combinatorial approach. The reaction kinetics, corresponding apparent rate constants k, and activation energies E_a, as well as activation entropies $\Delta S^{\ddagger}$, determined according to both approaches agree well with each other to within the experimental error. Hence, these parameters can be quantitatively determined using the described combinatorial approach. A comparison of the reactions of the two model systems indicated that the transition state is tighter for the acid-catalyzed ester hydrolysis in SAMs of the novel disulfide *t*-Bu-C10 compared to the hydrolysis of the ester groups in SAMs of NHS-C10 on gold.

Introduction

Coupling reactions for the activation or the passivation of surfaces are crucial steps in many applications in the fields of sensors, biomedical devices, and antifouling coatings, as well as high throughput screening and array technology.[1−3] Many approaches rely on monomolecular or thin organic films to covalently couple active species, such as receptors or protein-repellant polymers, to solid supports.[4] In many cases the reaction protocols must be optimized to ensure optimal surface coverages and (bio)-availability of the active components.

Typically, the reactivity of functional groups in organized layer architectures utilized in the corresponding coupling reactions is reduced compared to reactions occurring in solution.[5,6] The mentioned optimization of reaction conditions requires further systematic investigations of surface coverages and likely other relevant parameters, such as receptor orientation, clustering, and so forth. Unfortunately, the corresponding measurements are very time-consuming, because individual samples must be analyzed in a step-by-step fashion using very sensitive spectroscopic and microscopic methods.[7]

One promising approach to circumvent the inefficient sequential approach is the use of rapid parallel screening methodologies (also called combinatorial or high throughput screening approaches).[8] In particular the use of various gradients, among others composition,[9] temperature,[10] or film thickness gradients,[11] is a promising approach to overcome the shortcomings of traditional sequential screening.

Combinatorial and high-throughput experimentation has been widely applied in the fields of organic materials[12,13] inorganic materials,[14] and catalysis[15,16] as well as

* Corresponding author. E-mail: h.schonherr@tnw.utwente.nl. Tel.: ++31 53 489 3170. Fax: ++31 53 489 3823.

(1) (a) Fodor, S. P. A.; Read, J. L.; Pirrung, M. C.; Stryer, L.; Lu, A. T.; Solas, D. *Science* **1991**, *251*, 767. (b) Chee, M.; Yang, R.; Hubbell, E.; Berno, A.; Huang, X. C.; Stern, D.; Winkler, J.; Lockhart, D. J.; Morris, M. S.; Fodor, S. P. A. *Science* **1996**, *274*, 610.

(2) Multistep reactions on SAMs are a widely used way to synthesize DNA chips, see, for example, Pirrung, M. C. *Angew. Chem., Int. Ed.* **2002**, *41*, 1276.

(3) Schena, M. *Microarray Analysis*; Wiley-Liss, Wiley & Sons: Hoboken, NJ, 2003.

(4) (a) Case, M. A.; McLendon, G. L.; Hu, Y.; Vanderlick, T. K.; Scoles, G. *Nano Lett.* **2003**, *3*, 425. (b) Liu, G. Y.; Xu, S.; Qian, Y. *Acc. Chem. Res.* **2000**, *33*, 457. (c) Sigal, G. B.; Bamdad, C.; Barberis, A.; Strominger, J.; Whitesides, G. M. *Anal. Chem*. **1996**, *68*, 490. (d) Prime, K. L.; Whitesides, G. M. *Science* **1991**, *252*, 1164.

(5) (a) Neogi, P.; Neogi, S.; Stirling, C. J. M. *J. Chem. Soc.*, *Chem. Commun*. **1993**, 1134. (b) van Ryswyk, H.; Turtle, E. D.; Watson-Clark, R.; Tanzer, T. A.; Herman, T. K.; Chong, P. Y.; Waller, P. J.; Taurog, A. L.; Wagner, C. E. *Langmuir* **1996**, *12*, 6143. (c) Wang, J.; Kenseth, J. R.; Jones, V. W.; Green, J.-B. D.; McDermott, M. T.; Porter, M. D. *J. Am. Chem. Soc.* **1997**, *119*, 12796.

(6) For reviews see, for example, (a) Chechik, V.; Crooks, R. M.; Stirling, C. J. M. *Adv. Mater.* **2000**, *12*, 1161. (b) Sullivan, T. P.; Huck, W. T. S. *Eur. J. Org. Chem.* **2003**, *1*, 17.

(7) For recent reviews, see (a) Wirth, M. J. (guest editor). Chemical Analysis in Small Domains Special Issue. *Chem. Rev.* **1999**, *99* (10). (b) Vancso, G. J.; Hillborg, H., Schönherr, H. *Adv. Polym. Sci.* **2005**, *182*, in press.

(8) For recent reviews, see, for example, (a) Meredith, J. C.; Karim, A.; Amis, E. J. *MRS Bull.* **2002**, *27*, 330. (b) Special issue in *Macromol. Rapid Commun*. **2004**, *25* (1). (c) Amis, E. J. *Nat. Mater.* **2004**, *3*, 83.

(9) For a review, see Ruardy, T. G.; Schakenraad, J. M.; van der Mei, H. C.; Busscher, H. J. *Surf. Sci. Rep.* **1997**, *29*, 3.

(10) (a) Mao, H.; Yang, T.; Cremer, P. S. *J. Am. Chem. Soc.* **2002**, *124*, 4432. (b) Beers, K. L.; Douglas, J. F.; Amis, E. J.; Karim, A. *Langmuir* **2003**, *19*, 3935.

(11) (a) Richter, U. *Thin Solid Films* **1998**, *313−314*, 102. (b) Meredith, J. C.; Smith, A. P.; Karim, A.; Amis, E. J. *Macromolecules* **2000**, *33*, 9747.

(12) Briehn, C. A.; Schiedel, M. F.; Bonsen, E. M.; Schuhmann, W.; Bauerle, P. *Angew. Chem., Int. Ed.* **2001**, *40*, 4680.

10.1021/la046967o CCC: $30.25
Published on Web 04/09/2005

Scheme 1. Schematic of the Temperature Gradient Setup Used in This Study[a]

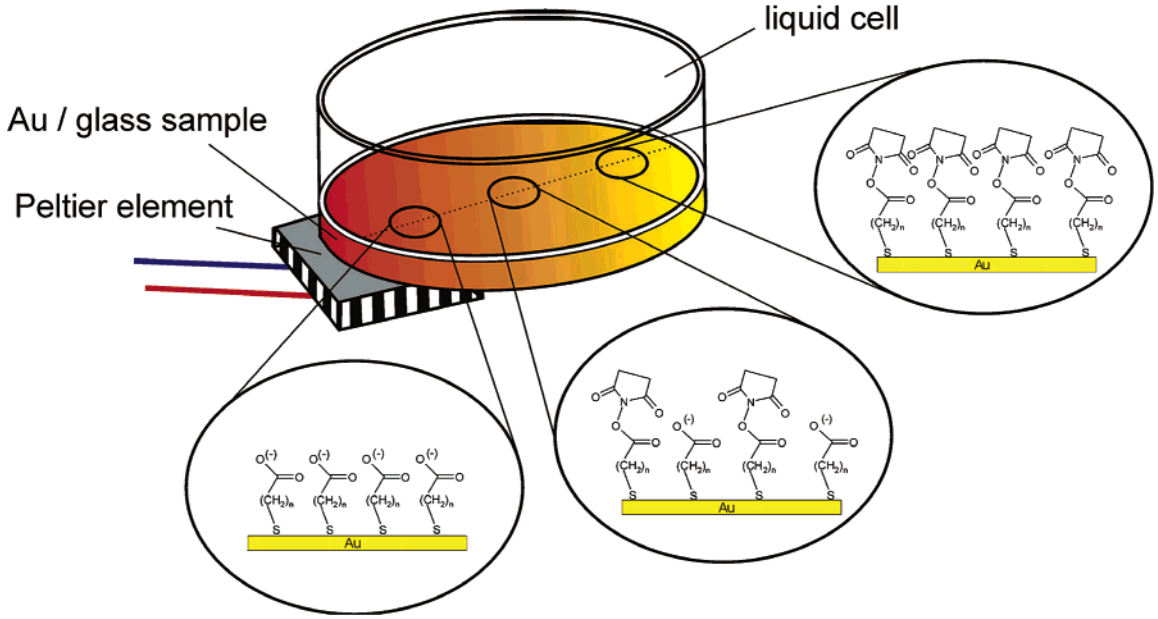

[a] A Peltier element is attached to the backside of a gold-covered glass substrate. On top of the substrate a closed liquid cell is mounted, which contains the reaction medium. The operation of the Peltier element establishes a temperature gradient along the sample (indicated by the color gradient), which, depending on the position on the sample surface, leads to different extents of the reaction after a given reaction time. As an example we show the hydrolysis of NHS ester groups in SAMs on gold. The position-resolved analysis of the surface composition of the thin organic film for a limited number of experiments with different reaction times yields the reaction kinetics and its dependence on temperature.

polymer research.[17,18] Owing to their relevance for biosensors and biochip arrays, self-assembled monolayer (SAM) platforms are a key area to be addressed in this context. Compositional or wettability gradients in SAMs have been reported for numerous applications, such as investigation of biomolecular interactions (e.g., protein adsorption and cellular interaction phenomena),[19] wetting,[20] high-throughput screening,[21] and microfluidics.[22] However, the use of gradients, and in particular thermal gradients, for the investigation of surface reactions in SAMs has not been reported yet.

In this paper we introduce a new combinatorial high throughput approach to quantitatively study reaction kinetics and its temperature dependence for surface reactions in organic thin films to circumvent the obvious limitations of the traditional point-by-point methods. The new approach is based on reactions carried out under a thermal gradient using a simple liquid cell−Peltier element design (Scheme 1). For the validation of the approach we studied the hydrolysis of NHS esters in SAMs of 11,11′-dithiobis(*N*-hydroxysuccinimidylundecanoate) (NHS-C10), which is well-known from previous studies [the corresponding second-order rate constant k'', e.g., at 30 °C is 4.5×10^{-2} M^{-1} s^{-1} and the apparent activation energy $E_a = 30$ kJ/mol and activation entropies $\Delta S_{298}^{\ddagger} = -184$ J/(mol K) have been recently reported],[23,24] and proceeded homogeneously down to molecular length scales.[25]

As reported in this paper, the thermal gradient established along the sample surface of a thin organic film can be exploited to rapidly study reaction kinetics and its temperature dependence *quantitatively* for surface and interfacial reactions in these films. On the basis of the example of the hydrolysis of a novel *t*-butyl ester-terminated disulfide, 11,11′-dithiobis(*tert*-butylundecanoate) (*t*-Bu-C10), the potential of the approach is demonstrated.

Experimental Section

Materials and Methods. NHS-C10 was available from previous studies,[23,24] and *t*-Bu-C10 was synthesized as described below. All the organic solvents, except for ethanol (Merck), were purchased from Biosolve and used as received. Concentrated HCl (37%) and all other reagents, unless mentioned otherwise, were purchased from Aldrich and used as received.

The Fourier transform infrared (FTIR) spectroscopy data were collected using a BIO-RAD model FTS575C FTIR spectrometer equipped with a liquid-nitrogen-cooled cryogenic mercury cadmium telluride detector. The ^{1}H NMR spectra were recorded on a Varian Unity Inova 300 spectrometer. ^{1}H NMR chemical shifts

(13) Schultz, P. G.; Xiang, X. D. *Curr. Opin. Solid State Mater. Sci.* **1998**, *3*, 153.
(14) Danielson, E.; Golden, J. H.; McFarland, E. W.; Reaves, C. M.; Weinberg, W. H.; Wu, X. D. *Nature* **1997**, *389*, 944.
(15) Senkan, S. M. *Nature* **1998**, *394*, 350.
(16) Reetz, M. T. *Angew. Chem., Int. Ed.* **2001**, *40*, 284.
(17) (a) Meier, M. A. R.; Schubert, U. S. *J. Mater. Chem.* **2004**, *14*, 3289. (b) Meredith, J. C.; Sormana, J. L.; Keselowsky, B. G.; Garcia, A.; Tona, A.; Karim, A.; Amis, E. J. *J. Biomed. Mater. Res.* **2003**, *66A*, 483.
(18) (a) Jandeleit, B.; Schaefer, D. J.; Powers, T. S.; Turner, H. W.; Wienberg, W. H. *Angew. Chem., Int. Ed.* **1999**, *38*, 2494. (b) Meredith, J. C.; Smith, A. P.; Karim, A.; Amis, E. J. *Macromolecules* **2000**, *33*, 9747. (c) Meredith, J. C.; Karim, A.; Amis, E. J. *Macromolecules* **2000**, *33*, 5760.
(19) Houseman, B. T.; Mrksich, M. *Chem. Biol.* **2002**, *9*, 443.
(20) (a) Chaudhury, M. K.; Whitesides, G. M. *Science* **1992**, *256*, 1539. (b) Daniel, S.; Chaudhury, M. K.; Chen, J. C. *Science* **2001**, *291*, 633.
(21) Meredith, J. C. *J. Mater. Sci.* **2003**, *38*, 4425.
(22) (a) Liedberg, B.; Tengvall, P. *Langmuir* **1995**, *11*, 3821. (b) Liedberg, B.; Wirde, M.; Tao, Y.-T.; Tengvall, P.; Gelius, U. *Langmuir* **1997**, *13*, 5329. (c) Elwing, H.; Welin, S.; Askendahl, A.; Nilsson, U.; Lundstrom, I. *J. Colloid Interface Sci.* **1987**, *119*, 203. (d) Elwing, H.; Golander, C.-G. *Adv. Colloid Interface Sci.* **1990**, *32*, 317. (e) Lee, J. H.; Kim, H. G.; Khang, G. S.; Lee, H. B.; Jhon, M. S. *J. Colloid Interface Sci.* **1992**, *151*, 563. (f) Morgenthaler, S.; Lee, S.; Zürcher, S.; Spencer, N. D. *Langmuir* **2003**, *19*, 10459. (g) Alexander, M. R.; Whittle, J. D.; Barton, D.; Short, R. D. *J. Mater. Chem.* **2004**, *14*, 408.
(23) Dordi, B.; Schönherr, H.; Vancso, G. J. *Langmuir* **2003**, *19*, 5780.
(24) Schönherr, H.; Feng, C. L.; Shovsky, A. *Langmuir* **2003**, *19*, 10843.
(25) (a) Dordi, B.; Pickering, J. P.; Schönherr, H.; Vancso, G. J. *Eur. Polym. J.* **2004**, *40*, 939. (b) Dordi, B.; Pickering, J. P.; Schönherr, H.; Vancso, G. J. *Surf. Sci.* **2004**, *570*, 57. (c) Schönherr, H.; Chechik, V.; Stirling, C. J. M.; Vancso, G. J. *J. Am. Chem. Soc.* **2000**, *122*, 3679.

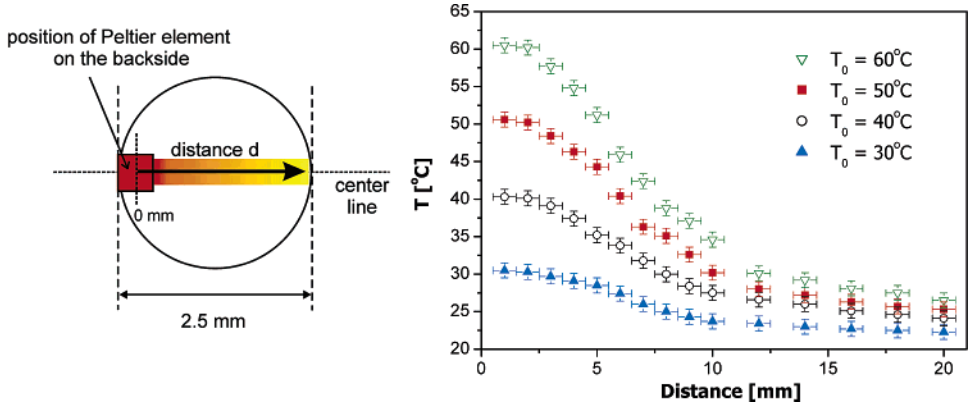

Figure 1. Left: Sample cell geometry in top view. Right: Temperature distribution along the sample surface, as measured by a thin thermocouple in air, for different temperatures T_0 at the position of the Peltier element (distance = 0 mm).

are stated relative to residual $CHCl_3$ (7.25 ppm). Fast-atom-bombardment mass spectrometry (FAB-MS) was carried out on a Finnigan MAT 90 spectrometer using *m*-nitrobenzyl alcohol or *o*-nitrophenyl octyl ether as a matrix. Elemental analyses were performed using a Carlo Erba EA1106.

Synthesis. *t-Bu-C10.* 11-Bromo-1-*tert*-butylundecanoate was prepared following a procedure adapted from ref 26. Concentrated sulfuric acid (0.55 mL, 10 mmol) was added to a vigorously stirred suspension of anhydrous magnesium sulfate (4.81 g, 40 mmol) in 40 mL of CH_2Cl_2. The mixture was stirred for 15 min, after which 11-bromo-undecanoic acid (10 mmol, 2.650 g) was added. Tertiary butanol (4.78 mL, 50 mmol) was added last, followed by stirring of the reaction mixture for 18 h at 25 °C. The mixture was then quenched with 75 mL of saturated sodium bicarbonate solution and stirred until all magnesium sulfate had dissolved. The solvent phase was separated, washed with brine, dried over $MgSO_4$, and concentrated to afford the crude product of 11-bromo-1-*tert*-butylundecanoate, which was purified by column chromatography; R_f (CH_2Cl_2) = 0.3. Isolated yield 2.57 g (80%), colorless oil.

^{1}H NMR (300 MHz, $CDCl_3$): δ 3.4 (t, 2H, J = 7.3 Hz, Br−CH_2), 2.18 (t, 2H, J = 7.3 Hz, CH_2COO), 1.82−1.61 (m, 4H, CH_2CH_2-CH_2), 1.42 (s, 9H, CH_3) 1.38−1.2 (m, 12H $CH_2CH_2CH_2$).

t-Bu-C10. Sodium thiosulfate (7 mmol, 1.737 g) was added to a solution of 11-bromo-1-*tert*-butylundecanoate (7 mmol, 2.247 g) in aqueous 50% 1,4-dioxane (20 mL). The mixture was heated at reflux for 2 h until the reaction to the intermediate salt was completed (clear solution). The oxidation to the corresponding disulfide was carried out in situ by adding iodine in portions until the solution retained a yellow to brown color after heating at 60 °C for 3 h. The excess of solid iodine was neutralized with 15% of sodium pyrosulfite in water. After removal of the solvent by rotary evaporation, the creamy suspension was filtered to yield the product. The crude product of *t*-Bu-C10 was purified by column chromatography; R_f (CH_2Cl_2) = 0.7. Isolated yield 0.92 g (48%), mp 37−39 °C.

^{1}H NMR (300 MHz, $CDCl_3$): δ 2.67 (t, 4H, J = 7.3 Hz, SCH_2), 2.18 (t, 4H, J = 7.3 Hz, CH_2COO), 1.82−1.61 (m, 8H, CH_2CH_2-CH_2), 1.42 (s, 18H, CH_3), 1.38−1.2 (m, 24H $CH_2CH_2CH_2$). Elem anal. Calcd. for $C_{30}H_{58}O_4S_2$ (546.3777 g/mol): C, 65.9; H, 10.7; S, 11.7. Found: C, 65.7; H, 10.7; S, 11.5. FAB-MS *m/z* 545.10 [M − H]; calcd for $C_{30}H_{58}O_4S_2$, 546.42. FTIR $\nu_{as}(CH_3)_{t-butyl}$ = 2978 cm^{-1}; $\nu_{as}(CH_2)$ = 2920 cm^{-1}; $\nu_s(CH_2)$ = 2852 cm^{-1}; ν(C=O) = 1730 cm^{-1}; δ_s $(CH_3)_{t-butyl}$ = 1391 cm^{-1}, 1368 cm^{-1}; ν(C−O) = 1253 cm^{-1}, 1154 cm^{-1}.

Monolayer Preparation. All glassware used to prepare monolayers was immersed in piranha solution [solution of 1:3 (v/v) 30% H_2O_2 and concentrated H_2SO_4] for 15 min and then rinsed with copious amounts of high-purity water (Millipore Milli-Q water). *Caution*: *Piranha solution should be handled with extreme caution; it has been reported to detonate unexpectedly.* Gold substrates (200 nm gold on 2 nm Ti primer on glass), acquired from SSENS bv (Hengelo, The Netherlands), were cleaned by oxygen plasma treatment (5 min, 30 mA, 60 mTorr using a SPI Supplies, Plasma Prep II), subsequently immersed in ethanol for 10 min to remove any possible oxide layer,[27] and immersed with minimal delay into 1.0 mM solutions of NHS-C10 or *t*-Bu-C10 in ethanol. The substrates were removed from solutions after >16 h of assembly time and rinsed extensively with ethanol and water to remove any physisorbed material. Finally, the samples were dried in a stream of nitrogen.

Contact Angles (CAs) Measurement. Static and dynamic CAs were measured on a CA microscope (Data Physics, OCA 15 Plus) with Millipore water as the probe liquid at room temperature and ambient humidity. A set of at least three different locations was averaged per sample. Samples exposing chemical (compositional) gradients were analyzed by sequentially placing water droplets of equal volume (1 μL) along the center line of the sample surface (spacing of the drops ~2 mm). Images of the static CAs were recorded digitally (for an example see Figure 5); the subsequent quantitative analysis was performed using an automated drop shape analysis software routine.

X-ray Photoelectron Spectroscopy (XPS). XPS spectra were recorded on a PHI Quantum 2000 Scanning ESCA microprobe using a 100-μm diameter/25 W monochromated X-ray beam (Al anode) scanned over a 700 μm × 300 μm area at a takeoff angle of 45°. Samples exposing chemical gradients have been evaluated using a multipoint (small spot) analysis routine. Atomic concentrations were determined by numerical integration of the relative peak areas using the Multipak software with supplied sensitivity factors [C(1s), 0.314; O(1s), 0.733; N(1s), 0.733; S(2p), 0.717].[28]

Determination of Reaction Kinetics. *Standard Point-by-Point Approach.* The hydrolysis of *t*-Bu-C10 ester SAMs was carried out by incubation of the corresponding sample for different reaction times in a thermostated aqueous 6.0 M solution of HCl at 20, 30, 40, and 50 °C.[29] Following the reaction, the samples were rinsed with 1 M NaOH, H_2O, and finally ethanol before they were dried in a nitrogen stream. The analysis of the reaction kinetics of the hydrolysis reactions of the ester groups in SAMs on gold was carried out as described previously[23,24] by (static) CA measurements.

Combinatorial Approach. Surface reactions were carried out on SAM-covered gold substrates in the presence of a temperature gradient using a simple reaction cell, as shown schematically in Scheme 1. The experimental setup consists of a Peltier element (type TEC1 C-24.0-5.0-23/78-xy; size 6 × 6 mm^2; Eureca Messtechnik GmbH, Germany) attached by glue (Pritt type Glue-it, Henkel, Germany) to the backside of a gold-covered glass substrate (Figure 1, left) and a home-built liquid cell. The operation of the Peltier element using a Delta Electronica Power Supply E030-1 (typical voltage of 1.2 V and current of 300 mA)

(26) Wright, S. W.; Hageman, D. L.; Wright, A. S.; McClure, L. D. *Tetrahedron Lett.* **1997**, *38*, 7345.

(27) Ron, H.; Rubinstein, I. *Langmuir* **1994**, *10*, 4566.

(28) Wagner, C. D.; Riggs, W. M.; Davis, L. E.; Moulder, J. F. In *Handbook of X-Ray Photoelectron Spectroscopy*; Muilenberg, G. E., Ed.; Perkin-Elmer Corporation: Eden Prairie, MN, 1979.

(29) Note of caution: HCl vapors are corrosive; for safety regulations consult appropriate literature, for example, Hommel, G. *Handbuch der gefährlichen Güter*; Springer-Verlag: Berlin, 2003 (the Peltier was shielded against HCl vapors).

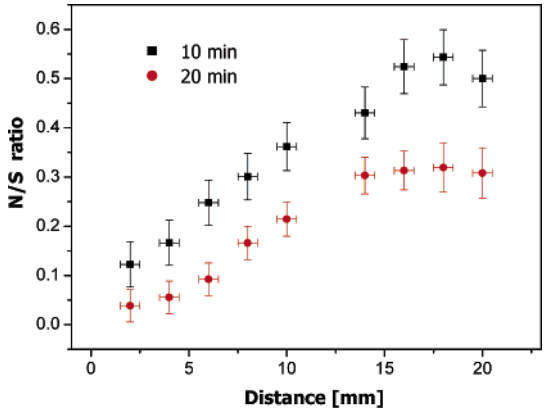

Figure 2. Position-resolved surface composition (N/S ratio) of SAMs of NHS-C10 following alkaline hydrolysis in 0.01 M NaOH for the indicated time determined from XPS measurements. The temperature of the reference point (distance 0 mm) was set to 60 °C.

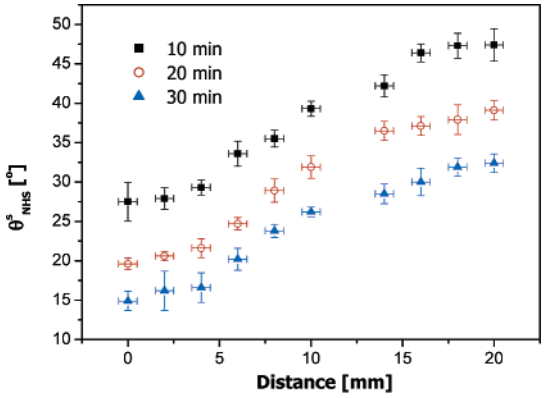

Figure 3. Static water CAs as a function of position following alkaline hydrolysis of SAMs of NHS-C10 in 0.01 M NaOH for the time indicated. The temperature of the reference point (distance 0 mm) was set to 60 °C.

establishes a temperature gradient along the sample surface. The surface temperature for operation in air was quantitatively determined using a thermocouple (Fluke 52 k/j thermometer, type J), as well as by determining the melting points of a range of carboxylic acids (Figure 1).[30] The surface reactions were carried out as follows: A volume of 0.25 mL of the reaction medium was pipetted into the liquid cell. The preheated substrate/Peltier assembly was then mounted onto the liquid cell. Following the surface reaction in an alkaline or acidic medium for a pre-set reaction time t, the substrate was removed from the cell and rinsed immediately according to the previously reported procedures[23,24] for hydrolysis of NHS ester groups or the procedure mentioned above for the hydrolysis of *tert*-butyl ester groups, respectively. The surface compositional gradient obtained was determined with minimal delay as a function of position along the center line of the sample by water CA measurements (see also Supporting Information, Figure S-1) and position-resolved small area XPS analysis (details see above).

Results and Discussion

The newly developed temperature gradient cell was tested in a first set of experiments to validate the combinatorial approach for the rapid acquisition of data that allows us to determine the reaction kinetics and estimate its temperature dependence. For this purpose we studied the well-characterized alkaline hydrolysis of NHS ester groups in SAMs of NHS-C10.[23,24]

Hydrolysis of NHS Esters in SAMs of NHS-C10. Following the base-catalyzed hydrolysis in 0.01 M NaOH for different reaction times, samples were analyzed by small area XPS analysis. Data points were taken with a lateral spacing of 2 mm along the center line (compare Figure 1). For all data points only the expected elements, that is, C, S, N, and O, as well as Au from the underlying substrate, were observed (see Supporting Information, Figure S-2). Figure 2 shows the N/S ratio calculated from the detailed XPS element scans for different positions along the center line.

A comparison with the temperature calibration depicted in Figure 1 shows a good qualitative agreement between surface temperature and decrease in nitrogen content of the surface layer sampled by XPS. The decrease in nitrogen content and, hence, loss of NHS ester groups is more pronounced at higher temperatures. As the temperature gradient along the sampled line is known (Figure 1), the extent of hydrolysis can be in principle determined quantitatively.[31] However, as area-selective XPS is a time-consuming technique[32] and because we have previously shown that CA measurements and the application of the Cassie equation allow one to rapidly determine the relative surface coverages that result from this reaction,[23,24] the analysis of the reaction kinetics will be based on CA measurements in the following sections.

The static CAs measured along the direction of the temperature gradient for NHS-C10 reacted in 0.01 M NaOH for 10, 20, and 30 min are summarized in Figure 3. The temperature of the reference point (distance 0 mm) was set to 60 °C.

Consistent with the XPS data shown in Figure 2, the CA measurements show a trend of more pronounced hydrophilicity in positions that correspond to higher reaction temperatures. The estimation of the relative surface coverages from the CA data was performed according to the Cassie equation.[33,34] An analysis of the data according to the Israelachvili−Gee equation[35,36] yield very similar results (see Supporting Information, Tables S-1 and S-2).

In Figure 4a the natural logarithm of the corresponding coverages is plotted versus the reaction time. For all reaction temperatures studied we observe a linear dependence, in accordance with previous work carried out by the standard point-by-point approach.[23,24] This linear behavior indicates that the hydrolysis of NHS ester groups proceeds homogeneously[25] and can be described by a standard pseudo-first-order kinetics.[23] The pseudo-first-order rate constants determined from linear least-squares fits correspond well to those reported previously for similar reaction temperatures (Table 1).[24] The second-order rate

(30) Schönherr, H.; Bailey, L. E.; Frank, C. W. *Langmuir* **2002**, *18*, 490.

(31) The temperature at the SAM−water interface was found (via the determination of the second-order rate constant at different surface temperatures and reaction times) to within the experimental error equal to the temperature calibration in air (Figure 1).

(32) Alternative approaches for the high throughput mapping of gradients have been reported. For example, (a) surface chemistry and molecular orientation using near-edge X-ray absorption fine structure spectroscopy, Fischer, D. A.; Efimenko, K.; Bhat, R. R.; Sambasivan, S.; Genzer, J. *Macromol. Rapid Commun.* **2004**, *25*, 141. (b) ToF-SIMS: Roberson, S. V.; Fahey, A. J.; Sehgal, A.; Karim, A. *Appl. Surf. Sci.* **2002**, *200*, 150.

(33) Cassie, A. B. D. *Discuss. Faraday Soc.* **1948**, *3*, 11.

(34) $\cos\theta_{exp} = \chi_{ester}\cos\theta_{ester} + \chi_{COOH}\cos\theta_{COOH}$, where χ_{ester} and χ_{COOH} are the surface coverages of the two components and $\theta_{ester} = 58°$ and $\theta_{COOH} = 15°$ are the static CAs of the surface composed of NHS ester and carboxyl groups, respectively.

(35) Israelachvili, J. N.; Gee, M. L. *Langmuir* **1989**, *5*, 288.

(36) $(1 + \cos\theta_{exp})^2 = \chi_{ester}(1 + \cos\theta_{ester})^2 + \chi_{COOH}(1 + \cos\theta_{COOH})^2$, where χ_{ester} and χ_{COOH} are the surface coverages of the two components and $\theta_{ester} = 58°$ and $\theta_{COOH} = 15°$ are the static CAs of the surface composed of NHS ester and carboxyl groups, respectively.

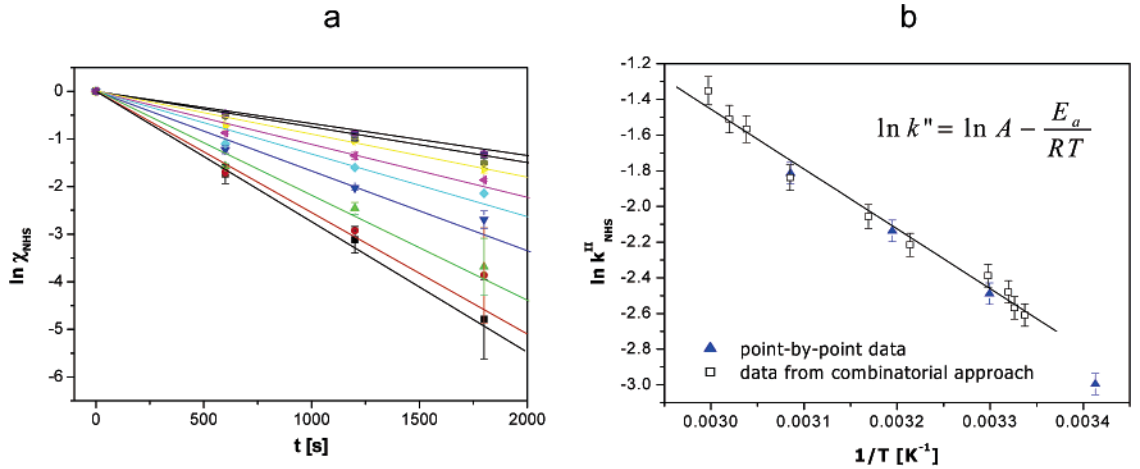

Figure 4. a. Linearization of the NHS ester surface coverage data calculated from the CA data using the Cassie equation according to pseudo-first-order kinetics for T between 25 °C and 60 °C (the solid lines correspond to linear least-squares fits of the data). b. Second-order rate constants obtained from part a linearized according to the Arrhenius equation (the solid line corresponds to a linear least-squares fit of the combinatorial data). The previously reported data acquired in a point-by-point manner have been overlaid in this figure.

Table 1. Second-Order Rate Constants of Acid-Catalyzed Hydrolysis of NHS-C10 Ester SAMs Obtained at Different Temperatures Using the Cassie Equation for the Combinatorial Approach and the Standard Approach

T, °C	$k'' \times 10^2$, L/(mol s) Cassie[a]	$k'' \times 10^2$, L/(mol s) Cassie[b]
20.0 ± 2.0		5.0 ± 0.2
25.5 ± 2.2	7.3 ± 0.1	
27.5 ± 2.2	7.7 ± 0.2	
28.1 ± 1.5	8.4 ± 0.2	
30.1 ± 1.0	9.1 ± 0.3	8.3 ± 0.2
38.0 ± 1.0	10.9 ± 0.2	11.8 ± 0.4[c]
42.4 ± 1.0	12.7 ± 0.2	11.8 ± 0.4[c]
51.1 ± 0.5	15.9 ± 0.3	16.3 ± 0.4
56.2 ± 0.5	20.9 ± 0.2	
58.0 ± 0.5	22.1 ± 0.2	
60.5 ± 0.5	25.9 ± 0.4	

[a] Combinatorial approach. [b] Standard approach. [c] Data were determined for 40 ± 1.5 °C.

constants calculated from the pseudo-first-order rate constants obey the Arrhenius equation, as shown in Figure 4b.

A very good correspondence was also observed for the value of the activation energy determined according to the Arrhenius equation. From the slope of the linearized plot an activation energy E_a of 28 ± 2 kJ/mol was estimated for the combinatorial approach, which is to within the experimental error equal to the data reported previously (30 ± 2 kJ/mol).[24]

By applying transition state theory, we can calculate the activation entropy $\Delta S^{\ddagger}$ of this hydrolysis reaction.[37]

$$\Delta S^{\ddagger} = R\left(\ln\frac{A}{T} - \ln\frac{k_b}{h} - 1\right) \qquad (1)$$

where R is the gas constant, A is the preexponential factor of the Arrhenius equation, T is the absolute temperature, k_b is the Boltzmann constant, and h is Planck's constant. The values obtained by both approaches are again identical to within the error: $\Delta S_{298}^{\ddagger}$ (standard) = −184 ± 4 J/(mol K) versus $\Delta S_{298}^{\ddagger}$ (combinatorial) = −180 ± 6 J/(mol K).

Hence, we can conclude at this point that the combinatorial high throughput method based on the thermal gradient cell provides accurate and very consistent data that is to within the experimental error undistinguishable from data obtained in the time-consuming point-by-point measurements.

The new method was then applied to the study of a surface reaction of a novel reactive SAM system on gold, namely, to the study of the hydrolysis of *tert*-butyl ester groups in SAMs of *t*-Bu-C10 in an acidic medium.

Hydrolysis of *tert*-Butyl Esters in SAMs of *t*-Bu-C10. SAMs of the novel disulfide *t*-Bu-C10 on gold were fully characterized, as shown in the Supporting Information (Scheme S-1, Figure S-3, and Tables S-3 and S-4). The reflection FTIR spectroscopy and the XPS, as well as the CA, data were consistent with the formation of monolayers, which possess conformationally slightly disordered alkyl chains and expose the *t*-butyl ester groups at the surface of the layer. Hydrolysis in aqueous 6 M HCl for 20 min in the presence of a thermal gradient produced a clear gradient in hydrophilicity, as shown in Figure 5.

The corresponding CA data for four reaction times are shown in Figure 6a. The further analysis of the experimental kinetic data was carried out analogously to the NHS ester hydrolysis (i.e., pseudo-first-order kinetics). In Figure 6b we present the linearized data of the corresponding coverages plotted versus reaction time. For all reaction temperatures studied by using the new combinatorial approach, a linear dependence was observed. The concentration-independent second-order rate constants k'' obtained by both methods for different temperatures are summarized in Table 2 (see also Table S-5, Supporting Information). A fair agreement can be seen between the absolute values of k'' obtained for 30, 40, and 50 °C by both methods.

The second-order rate constants calculated from the data acquired using the combinatorial approach obey the Arrhenius equation, as shown in Figure 7. From the slope of the linearized plot, an activation energy of 35 ± 2 kJ/mol can be estimated. This value agrees favorably with the value of 35 ± 2 kJ/mol calculated for data determined by the standard point-by-point approach (see also Supporting Information, Figure S-4 and Table S-5).

By applying transition state theory (eq 1) we can calculate the activation entropies $\Delta S_{298}^{\ddagger}$ of this hydrolysis reaction (Table 3). Again we observe a good correspondence between data obtained by the two different approaches.

The activation entropy $\Delta S_{298}^{\ddagger}$ for the *tert*-butyl ester hydrolysis is more negative compared to the hydrolysis of

(37) Atkins, P.; Paula, J. *Physical Chemistry*, 7th ed.; Oxford University Press: New York, 2002.

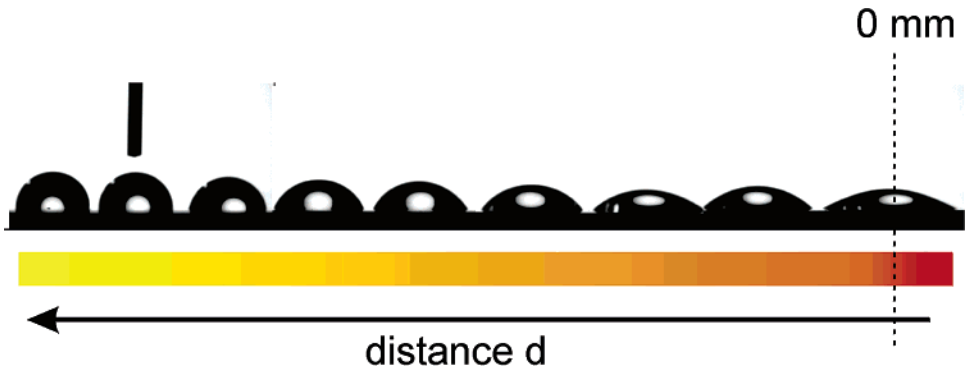

Figure 5. Collage of photographs showing the static water CAs on a SAM of *t*-Bu-C10 hydrolyzed in 6.0 N HCl for 20 min as function of position (image width 25 mm). The temperature of the reference point (located at distance $d = 0$ mm) was set to 60 °C. The thermal gradient and the reference point are schematically indicated.

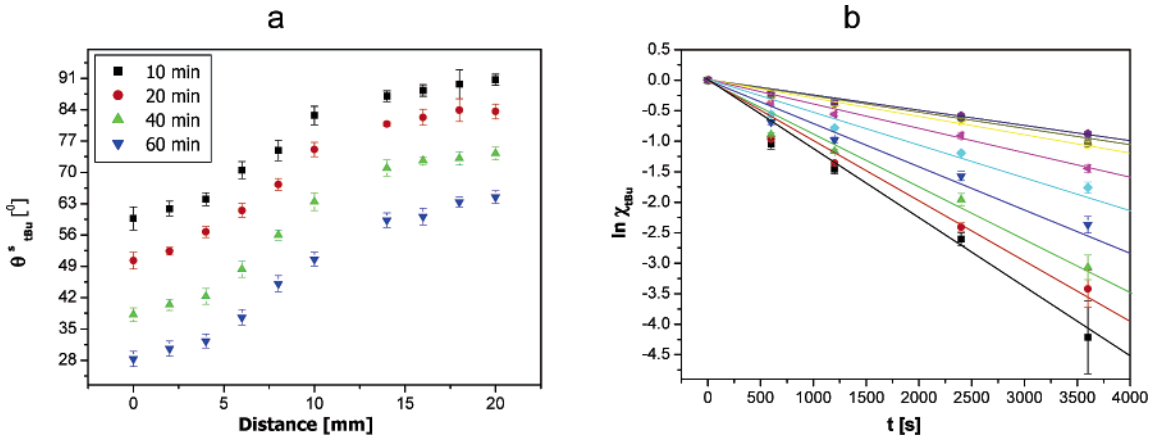

Figure 6. a. Experimental data of static water CAs on the *t*-Bu-C10 surface after reaction in the thermal gradient cell (temperature at the reference point was set to 60 °C). b. Linearization according to pseudo-first-order kinetics of the *t*-Bu ester surface coverage data calculated from the CA data for T between 25 °C and 60 °C using the Cassie equation. The solid lines correspond to linear least-squares fits of the data.

Table 2. Second-Order Rate Constants of Acid-Catalyzed Hydrolysis of *t*-Bu-C10 Ester SAMs Obtained at Different Temperatures Using the Cassie Equation for the Combinatorial Approach and the Standard Approach

T, °C	$k'' \times 10^2$, L/(mol s) Cassie[a]	$k'' \times 10^2$, L/(mol s) Cassie[b]
20.0 ± 2.0		3.3 ± 0.2
25.5 ± 2.2	4.1 ± 0.1	
27.5 ± 2.2	4.3 ± 0.2	
28.1 ± 1.5	4.7 ± 0.1	
30.1 ± 1.0	4.9 ± 0.3	5.4 ± 0.2
38.0 ± 1.0	6.7 ± 0.2	7.6 ± 0.3[c]
42.4 ± 1.0	8.5 ± 0.3	7.6 ± 0.3[c]
51.1 ± 0.5	11.2 ± 0.3	11.7 ± 0.4
56.2 ± 0.5	14.4 ± 0.2	
58.0 ± 0.5	15.9 ± 0.3	
60.5 ± 0.5	18.7 ± 0.3	

[a] Combinatorial approach. [b] Standard approach. [c] Data were determined for 40 ± 1.5 °C.

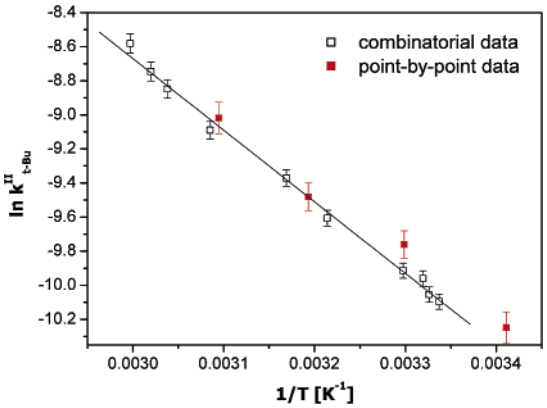

Figure 7. Second-order rate constants obtained from Figure 6b linearized according to the Arrhenius equation. The solid line corresponds to a linear least-squares fit of the combinatorial data. The data acquired in a point-by-point manner (see Supporting Information) have been overlaid in this figure.

the NHS ester, thus, indicating a tighter transition state.[38] Compared to model reactions in solution, which show a positive $\Delta S_{298}^{\ddagger}$ for the *tert*-butyl ester hydrolysis in an acidic medium,[39] the immobilization on the surface and likely also the tight packing of the terminal groups result in a sterically more demanding transition state. Compared to the NHS ester SAMs, the *tert*-butyl ester SAMs show a slightly better conformational ordering observed in the FTIR spectra (see Supporting Information, Figure S-3) and deduced in particular from the lower peak positions for the bands attributed to the asymmetric and symmetric C−H stretching vibrations of the CH_2 groups of the *tert*-butyl ester SAM ($\nu_a = 2920$ cm^{-1}, $\nu_s = 2851$ cm^{-1}) compared to the NHS ester SAM ($\nu_a = 2922$ cm^{-1}, $\nu_s = 2852$ cm^{-1}).

If the number of samples needed to obtain reliable data is taken into account, it becomes clear that the combinatorial approach based on thermal gradients leads to a reduction in experiments and samples by a factor of ~20. This improvement renders systematic investigations of reactivity and, hence, optimization of coupling reactions

(38) Hoffmann, R. W. *Aufklärung von Reaktionsmechanismen*; Thieme: Stuttgart, 1976; pp 32−44.
(39) Bunnett, J. F. *J. Am. Chem. Soc.* **1961**, *83*, 4956.

Table 3. Activation Energies and Activation Entropies Calculated on the Basis of Equation 1 of the Reactions Studied[a]

	E_a, kJ/mol	$\Delta S_{298}^{\ddagger}$, J/(mol K)
NHS Ester Hydrolysis		
standard approach	30 ± 2	-184 ± 4
combinatorial approach	28 ± 2	-180 ± 6
t-Butyl Ester Hydrolysis		
standard approach	35 ± 2	-221 ± 11
combinatorial approach	35 ± 2	-220 ± 3

[a] The analysis is based on surface coverages calculated according to the Cassie equation.

for a wide range of applications possible. This refers, for instance, to studies of the temperature dependence of surface reactions to obtain a better understanding of observed structure−property relationships.[23] In addition to monolayers on solid substrates, the combinatorial high throughput screening method developed can be easily expanded to address gas or solution phase surface and interface reactions in thin and ultrathin polymer films, which are attractive for coupling biologically relevant molecules to sensor or array platforms.[40]

Finally, the thermal gradient approach can be exploited further to *fabricate* defined surface *chemical*, that is, compositional, gradients. If appropriate surface reactions are chosen,[25] chemical gradients, which are homogeneous down to molecular length scales, can be fabricated.[41]

Conclusions

We have shown that thermal gradients can be exploited to quantitatively study reaction kinetics and its temperature dependence for surface and interfacial reactions in thin organic films on solid supports in a rapid manner. This new high throughput combinatorial approach is based on reactions carried out under a thermal gradient followed by position-resolved CA measurements and allows one to quantitatively determine the reaction kinetics, the corresponding apparent rate constants k, and activation energies E_a, as well as activation entropies $\Delta S^{\ddagger}$ on a very limited number of samples. A comparison of the reactivity of two model systems indicated that the alkaline ester hydrolysis of NHS-C10 SAMs on gold is hindered to a lower extent due to packing constraints of the ester groups compared to the acid-catalyzed ester hydrolysis in SAMs of the novel disulfide *t*-Bu-C10.

Acknowledgment. The authors would like to thank Prof. Dr. G. Julius Vancso for his continuous support and stimulating discussions. M.Sc. Chuanliang Feng and Dr. Barbara Dordi are acknowledged for fruitful discussions. This work has been financially supported by the Council for Chemical Sciences of The Netherlands Organization for Scientific Research (CW-NWO) in the framework of the *vernieuwingsimpuls* program.

Supporting Information Available: Static water CAs as a function of position, XPS spectra (survey scans), second-order rate constants, activation energies and entropies of acid-catalyzed hydrolysis determined according to Israelachvili−Gee, structure of novel disulfide *t*-Bu-C10, FTIR spectra, CAs, and XPS data of SAMs of *t*-Bu-C10 on gold, CA data and linearization for point-by-point data of the hydrolysis of *t*-Bu-C10, and second-order rate constants of acid-catalyzed hydrolysis of *t*-Bu-C10 according to Israelachvili−Gee. This material is available free of charge via the Internet at http://pubs.acs.org.

LA046967O

(40) Schönherr, H.; Feng, C. L.; Shovsky, A.; Degenhart, G.; Dordi, B.; Zhang, Z.; Förch, R.; Knoll, W.; Vancso, G. *J. PMSE Prepr.* **2004**, *90*, 689.

(41) Shovsky, A.; Salazar, R. B.; Vancso, G. J.; Schönherr, H. Manuscript in preparation.